

## Mutual Interference Mitigation for Multiple Connected Automotive Radar Systems

Arindam Bose , *Student Member, IEEE*, Bo Tang ,  
Mojtaba Soltanalian , *Senior Member, IEEE*,  
and Jian Li , *Fellow, IEEE*

**Abstract**—The number of commercial and civilian vehicles equipped with automotive radars is expected to rise rapidly in the forthcoming years and with that comes the problem of increased mutual interference between the radar sensors, which can result in severely reduced radar sensitivity and increased false alarm rates. The difficulty and complexity of the problem increase with MIMO radar systems and multiply even further with a growing number of vehicles present on the scene. A system of connected vehicles can efficiently address this problem by sharing information amongst themselves. In this paper, we propose an efficient waveform design algorithm that seeks to minimize a collective cross-ambiguity function. Vehicles that can talk to each other, can perform the design online in a collaborative manner, or offline, in which case the radar codes can be designed and stored in a codebook for future use. The proposed coding scheme is computationally efficient for practical use and the incorporation of such schemes requires only a slight modification of the existing systems. Our numerical examples indicate that the proposed scheme can significantly reduce the interference power level in a desired area of the radar cross-ambiguity functions.

**Index Terms**—Automotive radar systems, connected vehicles, MIMO, mutual interference mitigation, slow-time coding.

### I. INTRODUCTION

In recent years, automotive radars have become an essential part of the Adaptive Cruise Control (ACC) system in civilian and commercial vehicles towards safe and reliable autonomous vehicle operations combined with high-quality comfort features [1], [2]. The frequency modulated continuous wave (FMCW) [3]–[5] technique for signal propagation is widely used in automotive radars due to its excellent performance in high-resolution settings [6]–[8]. As a result, there is a strong appetite for mass production of FMCW-based radars, which in certain cases tend to be quite similar, or even identical [9]. Such an increasing number of similar radar systems on the road would lead to growing mutual interference, which in turn may result in severely reduced radar sensitivity [10], [11]. In the wake of this problem, it is inevitable to design FMCW radar systems that are robust to such mutual interference, or can mitigate it [12]–[15].

Manuscript received December 25, 2020; revised April 17, 2021 and July 22, 2021; accepted August 23, 2021. Date of publication August 30, 2021; date of current version October 15, 2021. This work was supported in part by U.S. National Science Foundation under Grants ECCS-1708509 and ECCS-1809225 and in part by Illinois Discovery Partners Institute (DPI) Seed Award. The review of this article was coordinated by Dr. Vuk Marojevic. The review of this article was coordinated by Dr. Vuk Marojevic. (*Corresponding author: Arindam Bose.*)

Arindam Bose and Mojtaba Soltanalian are with the Department of Electrical and Computer Engineering, University of Illinois at Chicago, Chicago, IL 60607 USA (e-mail: abose4@uic.edu; msol@uic.edu).

Bo Tang is with the Department of Electronic Engineering and Information Science, University of Science and Technology of China, Hefei 230027, China, and also with the Electronic Engineering Institute, Hefei 230000, China (e-mail: tangbo06@gmail.com).

Jian Li is with the Department of Electrical and Computer Engineering, University of Florida, Gainesville, FL 32611 USA (e-mail: li@dsp.ufl.edu).

Digital Object Identifier 10.1109/TVT.2021.3108714

Mutual interference in different radar systems is a longstanding problem and their corresponding mitigation techniques have been addressed many times in the literature [9], [16]–[23]. In [9], the authors address the mutual interference problem between two vehicles and proposed multiple coding schemes that aim to minimize the discrete periodic cross-ambiguity function (CAF) in a desired area for a single-input-single-output (SISO) scenario. The authors in [16] study the impact of radar waveform design and the associated receiver processing on the statistics of radar-to-radar interference and further propose an approach based on pseudo-random cyclic orthogonal sequences (PRCOS), which enable sensors to rapidly learn the interference environment and avoid using frequency overlapping waveforms. An iterative filtering algorithm followed by matched filtering for each radar has been suggested in [17] to suppress the radar-to-radar interferences. The references in [18]–[21] propose different types of transmissions to suppress the mutual interference between automotive radar systems.

The problem of mutual interference multiplies many-fold when several cars with similar or almost identical MIMO radar systems are in close proximity. A system of connected vehicles can be a blessing in such a scenario where the vehicles can agree on a certain set of transmit waveforms through sharing information amongst each other. In the not-so-far future, it is reasonable to expect that connected vehicles will go beyond academic pursuit and will be introduced to real-world smart-road networks. Many existing studies show the effectiveness of connected vehicles, and that transportation systems can be enhanced with more connected vehicles on the road [24]. In this paper, we consider the general scenario in which multiple cars, that are able to communicate and come to a consensus on the optimal radar waveforms to be shared among them. We thus extend the work of [9] to design such waveforms to suppress mutual interference in the case of similar or identical MIMO radar systems for multiple connected vehicles. An efficient design is possible when the vehicles are able to share information such as their dynamical properties and other radar parameters *e.g.*, number of transmit antennas, chirp parameters *etc.* Note that a distributed and mutually cooperative design protocol can be adopted for the online design of such waveforms in a collaborative manner. The design can also be done offline where shareable radar codes can be designed and stored in a centralized radar codebook for later usage.

### II. PROBLEM FORMULATION

Let us consider the scenario where  $V$  vehicles are present on the scene, all equipped with similar or almost identical MIMO radar systems having  $M_1, \dots, M_V$  antennas, respectively, each of which transmits *waveforms* of length  $N$ . Moreover, to keep the transmit power constant over the  $N$  pulses, we constrain the waveforms to be unimodular; meaning that the waveform elements emitted by a generic vehicle  $v$ , denoted as  $\{\mathbf{x}_{v,m}\}_{m=1}^{M_v} \in \mathbb{C}^N$ , are constrained to be on the unit circle, *i.e.*,  $|x_{v,m}(n)| = 1, \forall n$ .

In order to develop the signal model for the above scenario, we first consider a simple case with two vehicles equipped with similar SISO radar systems. In particular, we closely follow a signal model used in [9] that especially considers mutual interference mitigation in slow-time. The two similar radar systems operate within the same frequency band  $f_c$  and  $B/T_c$  ratio, where  $B$  and  $T_c$  are the FMCW signal bandwidth and chirp time, respectively. The complex periodic consecutive pulses transmitted by the two cars are  $\mathbf{x}_1 = [x_1(1), \dots, x_1(N)]^T$  and  $\mathbf{x}_2 = [x_2(1), \dots, x_2(N)]^T$ , respectively, where  $|x_1(n)| = |x_2(n)| = 1, \forall n$ , where  $(\cdot)^T$  denotes the transpose operator.

In order to mitigate the mutual interference between the two radars, a common approach is to make sure that the periodic cross-ambiguity function (PCAF) between  $\mathbf{x}_1$  and  $\mathbf{x}_2$  has small values in a range-Doppler region of interest [9], [25]–[27]. Given that the two radar systems usually have unsynchronized transmissions, the desired area should include all possible delays. Hence one can consider the following optimization problem:

$$\begin{aligned} \min_{\mathbf{x}_1, \mathbf{x}_2} \quad & \sum_{l=-(N-1)}^{N-1} \sum_{p=-P}^P |r_{lp}|^2 \\ \text{s.t.} \quad & |x_1(n)| = |x_2(n)| = 1, \forall n, \end{aligned} \quad (1)$$

where

$$r_{lp} = \sum_{n=1}^N x_1(n)^* x_2((n+l) \bmod N) e^{-j2\pi np/N_f} \quad (2)$$

is the PCAF between  $\mathbf{x}_1$  and  $\mathbf{x}_2$  with  $N < N_f$ ,  $0 < P < N_f$ ,  $N_f$  is the total number of discrete (Doppler) frequencies, the value of  $P$  is governed by the maximum Doppler frequency of interest [9], and  $(\cdot)^*$  represents the complex conjugate operator. Note that due to the considered data model, the optimization problem in (1) inherently suppresses the clutter and other RF interferences [28]. The above problem can be rewritten in a compact form as,

$$\begin{aligned} \min_{\mathbf{x}_1, \mathbf{x}_2} \quad & \sum_{l=-(N-1)}^{N-1} \sum_{p=-P}^P |\mathbf{x}_1^H \text{Diag}(\mathbf{f}_p) \mathbf{C}_l \mathbf{x}_2|^2 \\ \text{s.t.} \quad & |x_1(n)| = |x_2(n)| = 1, \forall n, \end{aligned} \quad (3)$$

where  $\mathbf{C}_l = \mathbf{C}_{-l}^T = \begin{bmatrix} \mathbf{0} & \mathbf{I}_{N-l} \\ \mathbf{I}_l & \mathbf{0} \end{bmatrix}$  is a circular shift matrix,  $[\mathbf{f}_p]_n = \exp(-j2\pi np/N_f)$ ,  $(\cdot)^H$  denotes the conjugate transpose operator,  $\mathbf{I}_N$  represents the identity matrix of size  $N \times N$ , the symbol  $\mathbf{0}$  denotes the all-zero vector/matrix of given size, and  $\text{Diag}(\cdot)$  denotes the diagonal matrix, whose diagonal elements are determined by the vector argument.

In a multiple-MIMO radar case, the mutual interference stems not only from the waveforms of a similar radar system nearby, but also from the various waveforms transmitted by the same radar system. Following the formulation in (3), firstly, the PCAF associated with the same radar system for all vehicles is given as,

$$Q_i = \sum_{l,p} \sum_{v=1}^V \sum_{m=1}^{M_v} \sum_{m'=1}^{M_{v'}} |\mathbf{x}_{v,m}^H \mathbf{A}_{l,p} \mathbf{x}_{v,m'}|^2 \quad (4)$$

where  $\mathbf{A}_{l,p} \triangleq \text{Diag}(\mathbf{f}_p) \mathbf{C}_l$  for  $l \in \{-N+1, \dots, N-1\}$  and  $p \in \{-P, \dots, P\}$ . Secondly, the PCAF for the codes emitted by all other vehicles is given as,

$$Q_o = \sum_{l,p} \sum_{v \neq v'} \sum_{m=1}^{M_v} \sum_{m'=1}^{M_{v'}} |\mathbf{x}_{v,m}^H \mathbf{A}_{l,p} \mathbf{x}_{v',m'}|^2. \quad (5)$$

Combining (4) and (5), the total PCAF to be minimized can be obtained as,

$$Q = Q_i + Q_o = \sum_{l,p} \sum_{v,v'} \sum_{m=1}^{M_v} \sum_{m'=1}^{M_{v'}} |\mathbf{x}_{v,m}^H \mathbf{A}_{l,p} \mathbf{x}_{v',m'}|^2. \quad (6)$$

By stacking the corresponding radar codes in matrix form and rewriting the above objective, we arrive at the criterion:

$$Q(\mathbf{X}_1, \dots, \mathbf{X}_V) = \sum_l \sum_p \sum_{v,v'} \|\mathbf{X}_v^H \mathbf{A}_{l,p} \mathbf{X}_{v'}\|_F^2 \quad (7)$$

where  $\{\mathbf{X}_v\}_{v=1}^V$  are radar code matrices, each containing the radar codes  $\{\mathbf{x}_{v,m}\}_{m=1}^{M_v}$  in its columns. Here,  $\|\cdot\|_F$  denotes the Frobenius norm of the matrix argument. Note that tackling (7) is difficult not only as the objective is *quartic* in radar codes  $\{\mathbf{X}_v\}_{v=1}^V$ , but also due to the fact that the number of PCAF values to be suppressed grows more quickly in terms of the problem dimension than the number of design variables.

In the following, we formulate a quadratic alternative to (6) that can be tackled more efficiently. One can partition the objective function in (6) in the following manner:

$$\begin{aligned} Q &= \sum_{l,p} \sum_{v=1}^V \sum_{m=1}^{M_v} |\mathbf{x}_{v,m}^H \mathbf{A}_{l,p} \mathbf{x}_{v,m}|^2 \\ &+ \sum_{l,p} \sum_{v=1}^V \sum_{m \neq m'}^{M_v} |\mathbf{x}_{v,m}^H \mathbf{A}_{l,p} \mathbf{x}_{v,m'}|^2 \\ &+ \sum_{l,p} \sum_{v \neq v'} \sum_{m=1}^{M_v} \sum_{m'=1}^{M_{v'}} |\mathbf{x}_{v,m}^H \mathbf{A}_{l,p} \mathbf{x}_{v',m'}|^2. \end{aligned} \quad (8)$$

It is interesting to observe that the quartic behavior of (8) particularly arises from self-interference terms  $\{\mathbf{x}_{v,m}^H \mathbf{A}_{l,p} \mathbf{x}_{v,m}\}$ , for all  $v \in \{1, \dots, V\}$  and  $m \in \{1, \dots, M_v\}$ . In order to recast the problem in a quadratic form [29], let

$$\mathbf{A}_{l,p}^r = \frac{1}{2}(\mathbf{A}_{l,p} + \mathbf{A}_{l,p}^H), \text{ and } \mathbf{A}_{l,p}^i = \frac{1}{2}(\mathbf{A}_{l,p} - \mathbf{A}_{l,p}^H). \quad (9)$$

Therefore, one can recast the first term of (8) as

$$\begin{aligned} & \sum_{l,p} \sum_{v=1}^V \sum_{m=1}^{M_v} |\mathbf{x}_{v,m}^H \mathbf{A}_{l,p} \mathbf{x}_{v,m}|^2 \\ &= \sum_{l,p} \sum_{v=1}^V \sum_{m=1}^{M_v} |\mathbf{x}_{v,m}^H \mathbf{A}_{l,p}^r \mathbf{x}_{v,m}|^2 + |\mathbf{x}_{v,m}^H j \mathbf{A}_{l,p}^i \mathbf{x}_{v,m}|^2 \\ &= \sum_{l,p} \sum_{v=1}^V \sum_{m=1}^{M_v} |\mathbf{x}_{v,m}^H (\mathbf{A}_{l,p}^r + \zeta \mathbf{I}_N) \mathbf{x}_{v,m} - \zeta N|^2 \\ &+ |\mathbf{x}_{v,m}^H (j \mathbf{A}_{l,p}^i + \zeta \mathbf{I}_N) \mathbf{x}_{v,m} - \zeta N|^2 \\ &= \sum_{l,p} \sum_{c \in \{r,i\}} \sum_{v=1}^V \sum_{m=1}^{M_v} |\mathbf{x}_{v,m}^H \tilde{\mathbf{A}}_{l,p}^c \mathbf{x}_{v,m} - \zeta N|^2 \end{aligned} \quad (10)$$

where

$$\tilde{\mathbf{A}}_{l,p}^r = \mathbf{A}_{l,p}^r + \zeta \mathbf{I}_N, \quad \tilde{\mathbf{A}}_{l,p}^i = j \mathbf{A}_{l,p}^i + \zeta \mathbf{I}_N$$

and  $\zeta \in \mathbb{R}$  is carefully selected such that  $\zeta > -\min(\bigcup_{l,p} \{\gamma_{\min}(\mathbf{A}_{l,p}^r), \gamma_{\min}(j \mathbf{A}_{l,p}^i)\})$  to ensure the positive definiteness of  $\{\tilde{\mathbf{A}}_{l,p}^c\}$  where  $\gamma_{\min}(\cdot)$  denotes the minimum eigenvalue of its matrix argument. Note that the quantity in (10) is still quartic with respect to (w.r.t.)  $\mathbf{x}_{v,m}$ . However, it is not difficult to verify that unit-norm vectors  $\mathbf{u}_{v,m,l,p}^c \in \mathbb{C}^N$  exist for which the above quantity becomes small if and only if the following alternative quantity becomes small:

$$\sum_{l,p} \sum_{c \in \{r,i\}} \sum_{v=1}^V \sum_{m=1}^{M_v} \left\| (\tilde{\mathbf{A}}_{l,p}^c)^{1/2} \mathbf{x}_{v,m} - \sqrt{\zeta N} \mathbf{u}_{v,m,l,p}^c \right\|_2^2, \quad (11)$$

where we have  $\|\mathbf{u}_{v,m,l,p}^c\|_2 = 1, \forall c, v, m, l, p$ . Observe that (11) is quadratic w.r.t.  $\mathbf{x}_{v,m}$ . This was made possible by a judicious over-parametrization. The resulting almost-equivalent minimization problem is presented in (12) at the bottom of this page.

Note that given the knowledge of the number of vehicles on the scene and the number of their corresponding MIMO antennas, (12) can be solved in an online manner. However, to enhance situational preparedness and further decrease the communication overhead, the codes can also be pre-designed offline and stored in a database for future use. Upon arriving into such situation, the vehicles just need to access their copy or download the codes from the said dataset before transmission. What comes next is an efficient algorithm to optimize (12).

### III. DESIGN OF OPTIMIZED WAVEFORMS

In order to efficiently tackle the problem in (12), we resort to an iterative cyclic optimization framework. Particularly, in  $s^{th}$  iteration, we separate each variable  $\{\mathbf{x}_{v,m}\}$ ,  $\{\mathbf{u}_{v,m,l,p}^r\}$ ,  $\{\mathbf{u}_{v,m,l,p}^i\}$ , and optimize the objective function (12) individually w.r.t. that variable, while fixing all other variables to their current values. This will lead to a monotonically decreasing collective PCAF until convergence is achieved. In the sequel, we drop the superscript ( $s$ ) for notational simplicity.

#### A. Optimization W.r.t. $\{\mathbf{x}_{v,m}\}_{v=1,m=1}^{V,M_v}$

We begin by reformulating the optimization problem in (12), shown at the bottom of this page w.r.t. each of  $\mathbf{x}_{v,m}$  for all  $v, m$ . The objective function in (12) then becomes what is described in (13), shown at the bottom of this page, or simply,

$$Q_{v,m} = \mathbf{x}_{v,m}^H \mathbf{R}_{v,m} \mathbf{x}_{v,m} + 2\Re\{\mathbf{x}_{v,m}^H \mathbf{s}_{v,m}\} + \text{const.} \quad (14)$$

where

$$\begin{aligned} \mathbf{R}_{v,m} = & \sum_{l,p} \sum_{m \neq m'}^{M_v} \mathbf{A}_{l,p} \mathbf{x}_{v,m'} \mathbf{x}_{v,m'}^H \mathbf{A}_{l,p}^H + \sum_{l,p} \sum_{c \in \{r,i\}} \tilde{\mathbf{A}}_{l,p}^c \\ & + \sum_{l,p} \sum_{v' \neq v} \sum_{m=1}^{M_v} \sum_{m'=1}^{M_{v'}} \mathbf{A}_{l,p} \mathbf{x}_{v',m'} \mathbf{x}_{v',m'}^H \mathbf{A}_{l,p}^H \end{aligned} \quad (15)$$

and  $\mathbf{s}_{v,m} = -\sqrt{\zeta N} \sum_{l,p} \sum_{c \in \{r,i\}} \sum_{m=1}^{M_v} (\tilde{\mathbf{A}}_{l,p}^c)^{H/2} \mathbf{u}_{v,m,l,p}^c$ . Here,  $\Re\{\cdot\}$  represents the real part of the complex argument. By dropping

the constant term in  $Q_{v,m}$ , the objective function can be reformulated as,

$$\begin{aligned} Q_{v,m} &= \mathbf{x}_{v,m}^H \mathbf{R}_{v,m} \mathbf{x}_{v,m} + 2\Re\{\mathbf{x}_{v,m}^H \mathbf{s}_{v,m}\} \\ &= \bar{\mathbf{x}}_{v,m}^H \mathbf{B}_{v,m} \bar{\mathbf{x}}_{v,m} \end{aligned} \quad (16)$$

where  $\bar{\mathbf{x}}_{v,m} \triangleq [\mathbf{x}_{v,m} \ 1]^T$ , and  $\mathbf{B}_{v,m} \triangleq \begin{bmatrix} \mathbf{R}_{v,m} & \mathbf{s}_{v,m} \\ \mathbf{s}_{v,m}^H & 0 \end{bmatrix}$ . Hence, the minimization of above w.r.t.  $\mathbf{x}_{v,m}$  is equivalent to the following,

$$\begin{aligned} \min_{\bar{\mathbf{x}}_{v,m}} & \bar{\mathbf{x}}_{v,m}^H \mathbf{B}_{v,m} \bar{\mathbf{x}}_{v,m} \\ \text{s.t.} & |x_{v,m}(n)| = 1, \quad n = 1, \dots, N, \\ & \bar{\mathbf{x}}_{v,m} = [\mathbf{x}_{v,m} \ 1]^T. \end{aligned} \quad (17)$$

As a result of the unimodular constraint on  $\mathbf{x}_{v,m}$ , the term  $\bar{\mathbf{x}}_{v,m}$  also has a constant  $\ell_2$ -norm, and hence, a diagonal loading of  $\mathbf{B}_{v,m}$  will not change the solution to the above problem [29]. Therefore, (17) can be rewritten in the following equivalent form:

$$\begin{aligned} \max_{\bar{\mathbf{x}}_{v,m}} & \bar{\mathbf{x}}_{v,m}^H \mathbf{D}_{v,m} \bar{\mathbf{x}}_{v,m} \\ \text{s.t.} & |x_{v,m}(n)| = 1, \quad n = 1, \dots, N, \\ & \bar{\mathbf{x}}_{v,m} = [\mathbf{x}_{v,m} \ 1]^T \end{aligned} \quad (18)$$

where  $\mathbf{D}_{v,m} \triangleq \gamma_{v,m} \mathbf{I}_{(N+1)} - \mathbf{B}_{v,m}$ , with  $\gamma_{v,m}$  being larger than the maximum eigenvalue of  $\mathbf{B}_{v,m}$ . Note that the above problem belongs to the family of UQPs [30], and can be efficiently tackled in an iterative manner using power-method-like iterations. For  $t$ -th internal iteration, the optimized code  $\mathbf{x}_{v,m}^{(t)}$  can be expressed as [29],

$$\hat{\mathbf{x}}_{v,m}^{(t)} = \exp \left\{ j \arg \left( \begin{bmatrix} \mathbf{I}_{N \times N} \\ \mathbf{0}_{1 \times N} \end{bmatrix}^T \mathbf{D}_{v,m} \bar{\mathbf{x}}_{v,m}^{(t-1)} \right) \right\} \quad (19)$$

where the iterations can be initialized with the latest design of  $\mathbf{x}_{v,m}$  (used as  $\mathbf{x}_{v,m}^{(0)}$ ).

---


$$\min \sum_{l,p} \sum_{v=1}^V \sum_{m \neq m'}^{M_v} |\mathbf{x}_{v,m}^H \mathbf{A}_{l,p} \mathbf{x}_{v,m'}|^2 + \sum_{l,p} \sum_{v \neq v'} \sum_{m=1}^{M_v} \sum_{m'=1}^{M_{v'}} |\mathbf{x}_{v,m}^H \mathbf{A}_{l,p} \mathbf{x}_{v',m'}|^2 + \sum_{l,p} \sum_{c \in \{r,i\}} \sum_{v=1}^V \sum_{m=1}^{M_v} \left\| (\tilde{\mathbf{A}}_{l,p}^c)^{1/2} \mathbf{x}_{v,m} - \sqrt{\zeta N} \mathbf{u}_{v,m,l,p}^c \right\|_2^2$$

s.t.  $\mathbf{x}_{v,m}$  are unimodular for all  $v, m$ ,

$$\|\mathbf{u}_{v,m,l,p}^c\|_2 = 1 \text{ for all } c, l, p, v, m. \quad (12)$$

---


$$\begin{aligned} Q_{v,m} = & \mathbf{x}_{v,m}^H \left( \sum_{l,p} \sum_{m \neq m'}^{M_v} \mathbf{A}_{l,p} \mathbf{x}_{v,m'} \mathbf{x}_{v,m'}^H \mathbf{A}_{l,p}^H \right) \mathbf{x}_{v,m} + \mathbf{x}_{v,m}^H \left( \sum_{l,p} \sum_{v' \neq v} \sum_{m=1}^{M_v} \sum_{m'=1}^{M_{v'}} \mathbf{A}_{l,p} \mathbf{x}_{v',m'} \mathbf{x}_{v',m'}^H \mathbf{A}_{l,p}^H \right) \mathbf{x}_{v,m} \\ & + \mathbf{x}_{v,m}^H \left( \sum_{l,p} \sum_{c \in \{r,i\}} \tilde{\mathbf{A}}_{l,p}^c \right) \mathbf{x}_{v,m} - 2\sqrt{\zeta N} \Re \left\{ \mathbf{x}_{v,m}^H \sum_{l,p} \sum_{c \in \{r,i\}} \sum_{m=1}^{M_v} (\tilde{\mathbf{A}}_{l,p}^c)^{H/2} \mathbf{u}_{v,m,l,p}^c \right\} + \text{const.} \end{aligned} \quad (13)$$

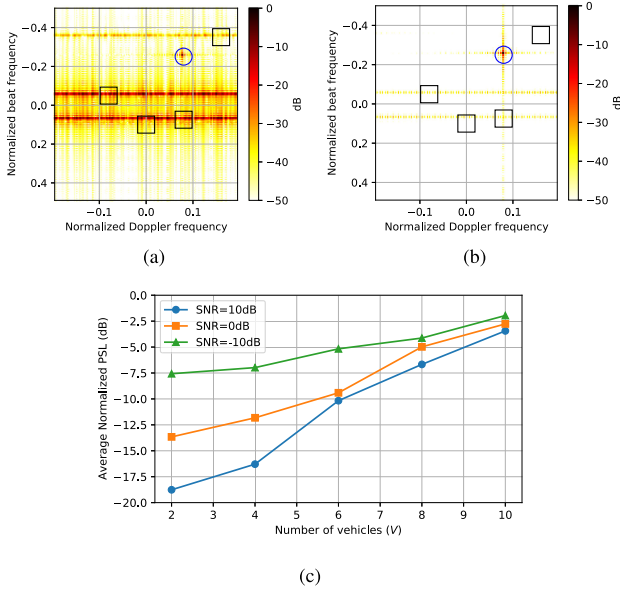


Fig. 1. The range-Doppler image (a) with random coding (b) with the optimized coding scheme. The blue circle is the target and black squares are the interfering vehicles. (c) Results of Monte Carlo simulation ( $n = 50$ ) showing average normalized peak sidelobe levels vs. number of vehicles ( $V$ ) for different target SNR scenarios.

### B. Optimization W.r.t. $\{\mathbf{u}_{v,m,l,p}^c\}$

Solving (12) w.r.t.  $\{\mathbf{u}_{v,m,l,p}^c\}$  for  $c \in \{r, i\}$  is immediate and resolves into the closed-form solution:

$$\hat{\mathbf{u}}_{v,m,l,p}^c = \frac{(\tilde{\mathbf{A}}_{l,p}^c)^{1/2} \mathbf{x}_{v,m}}{\|(\tilde{\mathbf{A}}_{l,p}^c)^{1/2} \mathbf{x}_{v,m}\|_2} \quad (20)$$

for all  $v, m, l, p$ . Notice that (20) can be done in parallel making the design process more agile. In the next section, we numerically examine the efficiency and applicability of the proposed algorithm.

## IV. NUMERICAL EXAMPLES AND DISCUSSIONS

In this section, we examine the effectiveness of the proposed method using several numerical experiments. In all experiments, we consider identical FMCW radar systems with the same carrier frequency of  $f_c = 24$  GHz and the bandwidth of the chirp signal is  $B = 150$  MHz. Furthermore, the sweep time is  $T_c = 50 \mu\text{s}$  and the number of periods within a CPI is  $N = 256$ . The considered data and clutter model in this paper follows from [9].

In the first experiment, we consider  $V = 5$  cars equipped with MIMO radar system, each capable of transmitting  $M_v = 4$  unimodular codes. We apply the optimized coding schemes to mitigate the mutual interference for these five identical radar systems operating in a typical scenario. The range of target as well as interfering cars are considered to be 50 m and  $\{70, 10, -20, -15\}$  m, respectively. The velocities associated with them are 10 m/s and  $\{20, -10, 0, 10\}$  m/s, respectively. Furthermore, the corresponding signal-to-noise ratios (SNR) are 10 dB and  $\{10, 30, 0, 60\}$  dB, respectively. One can observe that, the powers of the interference are much stronger than that of the target, which will lead to false alarm. The sampling frequency is  $f_s = 4$  MHz and  $M = 100$  samples are collected for each period. Fig. 1(a) shows the range-Doppler image of the scenario when a random code is used while that of the optimized code is shown in Fig. 1(b). It can be easily seen

from Fig. 1 that the interference power level is significantly reduced ( $> -20$  dB) and the target can be easily detected without suffering from false alarm issues.

In the next experiment, we perform a Monte Carlo simulation of designing codes for  $V = \{2, 4, 6, 8, 10\}$  vehicles in order to show the average performance of the algorithm. In particular, we simulate  $n = 50$  experiments for each of  $V$  having  $M = 4$  MIMO antennas and report the average normalized peak sidelobe level (PSL) of the PCAF for different target SNR =  $\{10, 0, -10\}$  dB, as depicted in Fig. 1(c). It is evident that as the number of vehicles grows large, it becomes more difficult to find codes with good interference mitigation capabilities, while the performance is satisfactory for a small number of vehicles. Furthermore, it is evident that the interference mitigation performance of the optimized codes improves as the SNR of the target increases. Note that, there may exist a fundamental limit on achievable interference mitigation when  $V$  grows large. However, from algorithmic point of view, there is no such limitation given unbounded resources to compute the optimized codes. Further note that, the proposed framework can be considered for designing sequences for ultra-wide band. In such a scenario, however, the radar code may be longer as one requires higher resolution, and thus each pulse length is required to be smaller.

## REFERENCES

- [1] M. Schneider, "Automotive radar: Status and trends," in *Proc. German Microw. Conf.*, 2005, pp. 144–147.
- [2] X. Yang, K. Zhang, T. Wang, and Y. Zhao, "Anti-interference waveform design for automotive radar," in *Proc. IEEE 2nd Adv. Inform. Technol., Electron. Automat. Control Conf.*, 2017, pp. 14–17.
- [3] D. Barrick and E. R. L. (U.S.), *FM/CW Radar Signals Digital Process. Environ. Res. Laborator.*, no. v. 55, 1973.
- [4] A. G. Stove, "Linear FMCW radar techniques," *IEE Proc. F - Radar Signal Process.*, vol. 139, no. 5, pp. 343–350, 1992.
- [5] I. Komarov, S. Smolskiy, and D. Barton, *Fundamentals of Short-Range FM Radar, Ser. Artech House Radar Library*. Boston, MA: Artech House, 2003. [Online]. Available: <https://books.google.com/books?id=m7spngEACAAJ>
- [6] G. S. Woods, D. L. Maskell, and M. V. Mahoney, "A high accuracy microwave ranging system for industrial applications," *IEEE Trans. Instrum. Meas.*, vol. 42, no. 4, pp. 812–816, Aug. 1993.
- [7] R. Stolle and B. Schiek, "Multiple-target frequency-modulated continuous-wave ranging by evaluation of the impulse response phase," *IEEE Trans. Instrum. Meas.*, vol. 46, no. 2, pp. 426–429, Apr. 1997.
- [8] B. Journet and G. Bazin, "A low-cost laser range finder based on an FMCW-like method," *IEEE Trans. Instrum. Meas.*, vol. 49, no. 4, pp. 840–843, Aug. 2000.
- [9] B. Tang, W. Huang, and J. Li, "Slow-time coding for mutual interference mitigation," in *Proc. IEEE Int. Conf. Acoust., Speech Signal Process.*, 2018, pp. 6508–6512.
- [10] F. Engels, P. Heidenreich, A. M. Zoubir, F. K. Jondral, and M. Wintermantel, "Advances in automotive radar: A framework on computationally efficient high-resolution frequency estimation," *IEEE Signal Process. Mag.*, vol. 34, no. 2, pp. 36–46, Mar. 2017.
- [11] I. Bilik, O. Longman, S. Villeval, and J. Tabrikian, "The rise of radar for autonomous vehicles: Signal processing solutions and future research directions," *IEEE Signal Process. Mag.*, vol. 36, no. 5, pp. 20–31, Sep. 2019.
- [12] S. H. Dokhanchi, B. S. Mysore, K. V. Mishra, and B. Ottersten, "A mmwave automotive joint radar-communications system," *IEEE Trans. Aerosp. Electron. Syst.*, vol. 55, no. 3, pp. 1241–1260, Jun. 2019.
- [13] S. Sedighi, B. Shankar, K. V. Mishra, and B. Ottersten, "Optimum design for sparse FDA-MIMO automotive radar," in *Proc. 53rd Asilomar Conf. Signals, Syst., Comput.*, 2019, pp. 913–918.
- [14] S. H. Dokhanchi, M. R. Bhavani Shankar, K. V. Mishra, and B. Ottersten, "Multi-constraint spectral co-design for colocated MIMO radar and MIMO communications," in *Proc. IEEE Int. Conf. Acoust., Speech Signal Process.*, 2020, pp. 4567–4571.
- [15] J. Huang *et al.*, "V2X-communication assisted interference minimization for automotive radars," *China Commun.*, vol. 16, no. 10, pp. 100–111, 2019.

- [16] S. Skaria, A. Al-Hourani, R. J. Evans, K. Sithamparanathan, and U. Parampalli, "Interference mitigation in automotive radars using pseudo-random cyclic orthogonal sequences," *Sensors (Basel, Switzerland)*, vol. 19, no. 20, Oct. 2019, Art no. 4459.
- [17] W.-Q. Wang and H. Shao, "Radar-to-radar interference suppression for distributed radar sensor networks," *Remote Sens.*, vol. 6, no. 1, pp. 740–755, 2014.
- [18] M. Goppelt, H. L. Blöcher, and W. Menzel, "Automotive radar - investigation of mutual interference mechanisms," *Adv. Radio Sci.*, vol. 8, pp. 55–60, Sep. 2010.
- [19] M. Goppelt, H. L. Blöcher, and W. Menzel, "Analytical investigation of mutual interference between automotive FMCW radar sensors," in *Proc. German Microw. Conf.*, 2011, pp. 1–4.
- [20] A. Bourdoux, K. Parashar, and M. Bauduin, "Phenomenology of mutual interference of FMCW and PMCW automotive radars," in *Proc. IEEE Radar Conf.*, 2017, pp. 1709–1714.
- [21] M. A. Hossain, I. Elshafiey, and A. Al-Sanie, "Mutual interference mitigation in automotive radars under realistic road environments," in *Proc. 8th Int. Conf. Inform. Technol.*, 2017, pp. 895–900.
- [22] C. Aydogdu *et al.*, "Radar interference mitigation for automated driving: Exploring proactive strategies," *IEEE Signal Process. Mag.*, vol. 37, no. 4, pp. 72–84, Jul. 2020.
- [23] G. M. Brooker, "Mutual interference of millimeter-wave radar systems," *IEEE Trans. Electromagn. Compat.*, vol. 49, no. 1, pp. 170–181, Feb. 2007.
- [24] X. Yang and M. Ji, *Connected vehicle system design for signalized arterials*, Univ. Utah, 2019. [Online]. Available: [https://nitc.trec.pdx.edu/research/project/1235/Connected\\_Vehicle\\_System\\_Design\\_for\\_Signalized\\_Arterials](https://nitc.trec.pdx.edu/research/project/1235/Connected_Vehicle_System_Design_for_Signalized_Arterials)
- [25] A. Aubry, A. De Maio, B. Jiang, and S. Zhang, "Ambiguity function shaping for cognitive radar via complex quartic optimization," *IEEE Trans. Signal Process.*, vol. 61, no. 22, pp. 5603–5619, Nov. 2013.
- [26] C.-Y. Chen and P. Vaidyanathan, "MIMO radar ambiguity properties and optimization using frequency-hopping waveforms," *IEEE Trans. Signal Process.*, vol. 56, no. 12, pp. 5926–5936, Dec. 2008.
- [27] H. He, P. Stoica, and J. Li, "On synthesizing cross ambiguity functions," in *Proc. IEEE Int. Conf. Acoust., Speech Signal Process.*, 2011, pp. 3536–3539.
- [28] M. M. Naghsh, M. Soltanalian, P. Stoica, M. Modarres-Hashemi, A. De Maio, and A. Aubry, "A doppler robust design of transmit sequence and receive filter in the presence of signal-dependent interference," *IEEE Trans. Signal Process.*, vol. 62, no. 4, pp. 772–785, Feb. 2014.
- [29] H. Hu, M. Soltanalian, P. Stoica, and X. Zhu, "Locating the few: Sparsity-aware waveform design for active radar," *IEEE Trans. Signal Process.*, vol. 65, no. 3, pp. 651–662, Feb. 2017.
- [30] M. Soltanalian and P. Stoica, "Designing unimodular codes via quadratic optimization," *IEEE Trans. Signal Process.*, vol. 62, no. 5, pp. 1221–1234, Mar. 2014.